

On a measurement of atmospheric stopping muons and neutron fluxes

Antonio Bonardi ^{a) b)}, Marco Aglietta ^{b)}, Gianmarco Bruno ^{b) c)},
Walter Fulgione ^{b)}, Ana Amelia Bergamini Machado ^{d)} and Amanda Porta ^{b)}

^{a)}Università di Torino, Italy

^{b)}INAF-IFSI Torino, Italy

^{c)}Università de L'Aquila, Italy

^{d)}INFN-Laboratori Nazionali del Gran Sasso, Italy

Abstract. A 1.5 m³ scintillator detector has been provided with an active muon veto to study the atmospheric stopping muon and neutron fluxes.

The detector, located in the INFN Gran Sasso National Laboratory external site (42° 25' 11" N, 13° 31' 2" E, altitude 970 m a.s.l.), consists of 1.2 tons of 0.1% Gd doped liquid scintillator viewed by 3 photomultipliers. The measurement has been done by sampling the waveforms of detector's pmts in time windows 20 and 100 μ s long: muon decay and neutron captures in the liquid scintillator allow disentangling stopping muons and neutrons signals from the rest of background.

The following results have been obtained: the stopping muons rate $R_{\mu}(E \geq 10 \text{ MeV}) = 13.89 \pm 0.30(\text{stat.}) \pm 0.04(\text{syst.}) \text{ ev s}^{-1}$, the muon mean life equal to $2.125 \pm 0.015 \mu\text{s}$ and the neutron flux $\Phi_{\text{neutron}}(E \geq 10 \text{ MeV}) = 75 \pm 8 \text{ neutron s}^{-1} \text{ m}^{-2}$.

Keywords: Neutrons, stopping muons

I. DETECTOR SETUP AND CALIBRATION

Atmospheric neutrons and stopping muons are large component of the background for a surface detector.

A liquid scintillator detector (1.5m x 1m x 1m, total active mass 1.2 tons) located in the Laboratori Nazionali del Gran Sasso (LNGS) Mounting Hall has been used to study the atmospheric neutrons and stopping muons fluxes.

The detector has been provided of a 4π active muon veto made by modules of plastic scintillator (7 panels 3 cm thick form lateral and bottom modules; 2 panels 2 cm thick are partially superimposed to form the top module) equipped with 27 2-inches XP2020 fast pmts. Each wall of the veto individually participates to the general trigger allowing to select different candidates: through-going muons, stopping-muons and neutrons.

The detector, filled with 0.1% Gd doped *white spirit* scintillator [1] and [2], is monitored by three 5-inches XP3550B pmts; the veto is connected to a majority which gives a pulsed signal proportional to the number of triggered modules. The waveforms outcoming from the three pmts of the detector and from the veto are sampled by a TDS5054B 4-channels digital oscilloscope

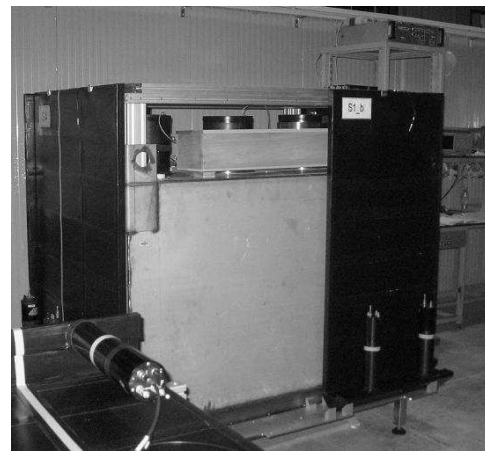


Fig. 1. The detector in the veto assembling phase

at 625 MSample/s (i.e. 1.6 ns for sampled bin). For each waveform the pre-trigger is used to evaluate the baseline value and its fluctuations which are used to set threshold's value for each channel. An event is considered "vetoed" if it occurs inside a time window 400 ns wide, centered at the time of occurrence of the veto signal.

Energy calibration of the detector has been got before each measurement by the signals of vertical muons selected by a muon telescope consisting of two plastic scintillator, one (20 X 20 cm²) located above and the other one (36 X 36 cm²) located under the detector.

The energy calibration procedure consists on:

1. the trigger is done by the coincidence between the signals of the 2 modules of the muon telescope inside a time window 200 ns long;
2. the three signals of detector's pmts are sampled by the oscilloscope in a time window 800 ns long;
3. on all the three channels the first 200 ns of each time window are used to evaluate the baseline and its fluctuation: after that, the muon signal is found by the 3-fold coincidence (threshold 3σ baseline's fluctuation, time interval 16 ns) and integrated;
4. after saturated signals rejection, the charge distribution was fitted by the convolution between a

- Gaussian and a Landau function: the peak of that function is the energy calibration parameter Q_{data} ;
- the second calibration parameter is the released energy by selected muons: it has been provided by Geant4 simulation of the detector and it has been found $E_{dep_{sim}} = 160$ MeV;
 - the energy calibration factor is given by the ratio $\frac{E_{dep_{sim}}}{Q_{data}}$.

Since $\left(\frac{\sigma_{E_{dep_{sim}}}}{E_{dep_{sim}}}\right)^2 \sim 2\%$ and $\left(\frac{\sigma_{Q_{data}}}{Q_{data}}\right)^2 \sim 1\%$, the systematic energy's uncertainty, due to calibration, is equal to $\sim 2.5\%$.

II. BACKGROUND SPECTRUM

The background spectrum has been measured by collecting the three pmts signals and the veto by the digital oscilloscope in randomly triggered gates $100 \mu s$ long. Events are defined by 3-fold coincidences among the three pmts of the counter (threshold = baseline + 3σ baseline's fluctuation, time interval 16 ns) and integrated in a gate 450 ns long.

We have acquired $230,274$ gates corresponding to about 22 second of real time. The vetoed and the un-vetoed components of the cumulative integral background spectrum are reported in fig.2.

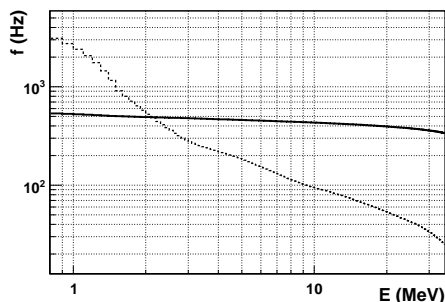


Fig. 2. Cumulative background spectrum: vetoed component (continuous line), un-vetoed component (dotted line)

The rate of vetoed events is:

$$R_{veto}(E \geq 10 \text{ MeV}) = 432 \pm 5(\text{stat}) \pm 1(\text{syst}) \text{ counts} \cdot \text{s}^{-1},$$

while the rate of un-vetoed events is:

$$R_{unveto}(E \geq 5 \text{ MeV}) = 182 \pm 3(\text{stat}) \pm 6(\text{syst}) \text{ counts} \cdot \text{s}^{-1}.$$

These rates are used in the next sections to normalize observed neutrons and stopping muons rates.

III. THE STOPPING MUONS RATE

Since the vetoed background rate has been measured, the next task is to know the fraction of stopping muons over the total number of vetoed events. The measurement setup is here summarized:

- the trigger condition is done by vetoed signals releasing inside the detector an energy above 4.5 MeV;
- the signals of the three detector's pmts and the veto are collected by the digital oscilloscope in acquisition windows $20 \mu s$ long after each trigger.

The first $2.4 \mu s$ before the trigger occurrence are used to evaluate the baseline on each channel and its fluctuations, the last $17.6 \mu s$ are used to look for muon and electron-positron signals;

- energy cuts:
 - prompt signals are required to be vetoed and corresponding to a released energy above 10 MeV;
 - delayed signals are required to be un-vetoed with a delay respect to the prompt 466 ns $\leq \Delta t < 10 \mu s$ and a released energy $10 \text{ MeV} < E < 60 \text{ MeV}$.

The low energy region ($E < 10$ MeV) of the delayed un-vetoed signals has been discarded during the data analysis because it is contaminated by the muon induced background (i.e. "after pulse" signals, neutron capture's signals due to neutrons present in the EAS, Extensive Air Shower) and it is not useful for muon decay signals investigation. A proof of this is the fact that the signals time delay distribution (fig.3) in this energy region can be divided into three parts: the after pulse peak for $\Delta t < 2 \mu s$, a not so evident μ -decay exponential for $2 \mu s < \Delta t < 5 \mu s$, and for $\Delta t > 5 \mu s$ the background component with a slight slope probably due to neutron capture.

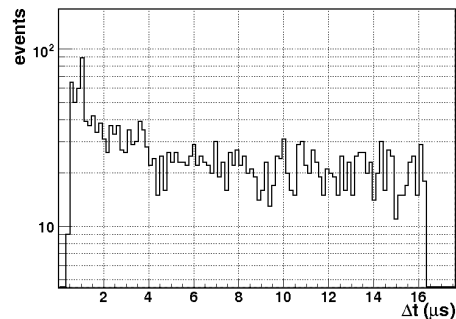


Fig. 3. $3 \text{ MeV} < E < 10 \text{ MeV}$ un-vetoed delayed time distribution

Applying the data analysis cuts previously explained, we have collected $229,897$ vetoed signals of energy above 10 MeV and $5,223$ delayed signals (~ 200 random coincidences are expected by Poisson background). The released energy spectra of all the triggered events and of stopping muon candidates are shown in fig.4. In fig.5 the energy spectrum of delayed signals without any energy cuts is shown; for comparison, the simulated Michel spectrum and background one normalized to the same live time are shown too.

After subtracting only the random coincidence and normalizing to the vetoed events rate, the observed stopping muon rate for $E_{\mu} > 10$ MeV is $9.43 \pm 0.17(\text{stat.}) \pm 0.05(\text{syst.}) \mu\text{-stop} \text{ s}^{-1}$.

The efficiency for the energy cuts obtained by the Monte Carlo simulation is: $\epsilon_E = 85.5 \pm 1.0 \pm 0.5\%$; whereas the

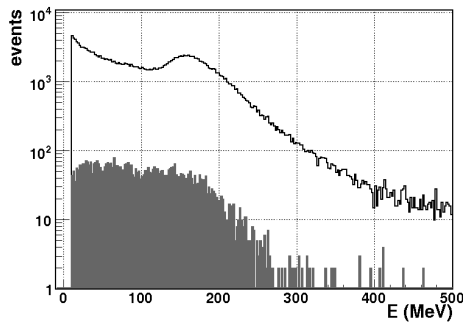


Fig. 4. Energy spectra of all triggers (black) and μ -stop candidates (grey filled)

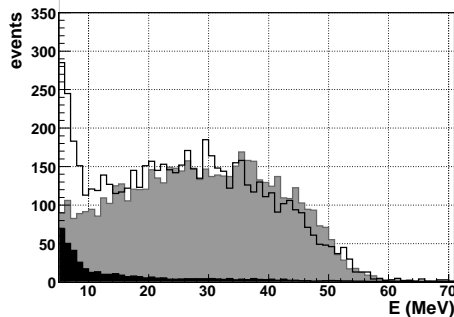


Fig. 5. Energy spectra of un-vetoed delayed events (black), Michel simulated (grey filled), normalized background (black filled)

efficiency for the finite time window is

$$\epsilon_t = \int_{t_1=466ns}^{t_2=10\mu s} \frac{e^{-t/\tau}}{\tau} dt = 79.4\%$$

for $\tau = 2.125 \pm 0.015 \mu s$ (see next section).

Therefore, having corrected the result for these two efficiency values, the stopping muons absolute rate for $E_\mu > 10$ MeV is expected to be equal to $13.89 \pm 0.30(stat.) \pm 0.04(syst.)$ events $\cdot s^{-1}$.

IV. MUON MEAN LIFE

For measuring the muon mean life's inside the liquid scintillator it was extremely important to have a very large statistics and, consequently, to maximize the trigger efficiency in rejecting background. For this reason the trigger has been modified by introducing the request that only one module of the veto system (corresponding to one wall of the parallelepiped) were hit ("single-triggering events"). In this way most of the thorough-going muons was rejected while the DAQ setup and data analysis held steady to the previous case. This trigger is more efficient in rejecting through-going muons and so in saving data acquisition time, but it rejects also stopping-muons inside EAS: this is the reason why it has not been used for the previous measurement.

We have collected 580,160 "single-triggering events" of energy above 10 MeV and found 76,403 selected delayed signals (~ 500 random coincidences are expected by Poisson background).

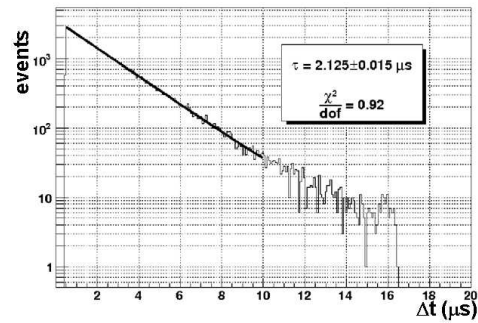


Fig. 6. Muon's decay candidates time distribution

In fig.6 the μ -decay candidate signals delay distribution is reported together with an "exponential + constant" fit. The so obtained muon mean life's value is $\tau = 2.125 \pm 0.015 \mu s$.

V. ATMOSPHERIC NEUTRONS RATE

The last goal of the work is to know the fraction of the atmospheric neutrons over the total number of un-vetoed events and to give an estimation of the atmospheric neutron's flux. A neutron incoming into the detector can give rise to a double signal: the first one due to a recoiling proton elastically scattered by the neutron, the second one due to neutron's capture on a Gd nucleus within a short time delay (the neutron capture's mean time in this detector has been measured [2] and it is $\sim 25 \mu s$). The measurement setup is here summarized:

1. the trigger is given by all un-vetoed events;
2. each trigger determines the acquisition of waveforms during $100 \mu s$: the first $5 \mu s$ are used to evaluate the baseline of each channel and to observe the prompt signal, the remaining $95 \mu s$ are used to look for delayed signals;
3. the prompt signals are requested to be un-vetoed with visible energy greater than 5 MeV; un-vetoed delayed signals are searched in the energy range of $3 \text{ MeV} < E < 10 \text{ MeV}$ and with a time delay respect to the corresponding prompt signal below $95 \mu s$;
4. since for this measurement it is extremely important to have a large dynamic energy range, instead of the three pmts single signals, the sum of them is sent to a linear fan out which output has been sent to three oscilloscope channels set at different scales. The assigned energy value for each event is the one given by the most precise non-saturated scale;
5. it is not anymore possible during data analysis to select events by 3-fold coincidence among pmts: that means an increase of the background rate for $E < 5$ MeV. For this reason, the threshold value is increased to 4 time the standard deviation of the baseline fluctuations.

During about 100 hours of data taking, we have collected 90,991 un-vetoed prompt signals with visible energy above 5 MeV, 8,190 of them are followed by at

least one un-vetoed delayed signal ($\sim 2,400$ are expected from random coincidences by Poisson background). In fig.7 are reported the un-vetoed delayed signal's energy spectrum together with the expected background and their difference (since the data acquisition setup has been changed, it has been performed another "ad hoc" background measurement). In fig.8 their time delay distribution is shown. The agreement between these results and the expected ones due to neutron captures in this detector is very good.

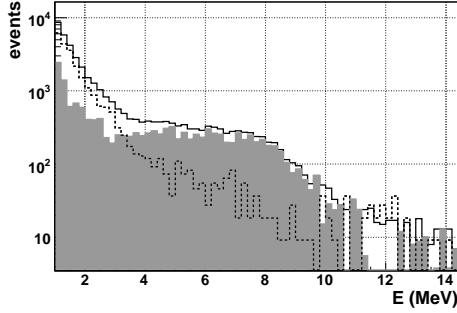


Fig. 7. Un-vetoed delayed signals (black continuous line), expected background (black dashed line), un-vetoed delayed signals without background (grey filled)

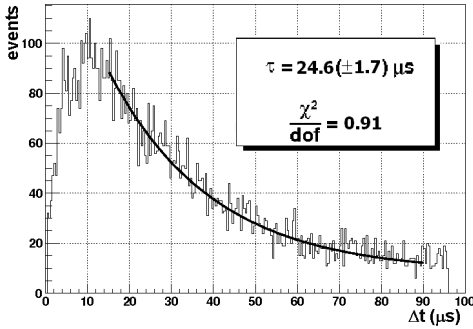


Fig. 8. Neutron capture candidates time delay distribution

Subtracting the random coincidence and normalizing to the un-vetoed events rate, the observed neutron rate for $E_{vis} > 5$ MeV is 11.69 ± 0.26 (stat.) ± 0.71 (syst.) neutron s^{-1} .

In order to obtain the real neutron flux we have to correct the experimental rate:

1. by taking into account the quenching effect of *white-spirit* liquid scintillator for recoiling protons;
2. by taking into account the trigger efficiency (i.e. the neutron capture detection's efficiency and the probability for an incoming neutron to be captured);
3. by scaling the neutron rate to the detector's acceptance.

In *white-spirit* based liquid scintillator, the quenching factor for 10 MeV protons is estimate to be ~ 2 and for 20 MeV protons ~ 1.5 . The neutron capture detection

efficiency has been estimate by a Geant4 simulation to be equal to $\sim 55\%$ whereas the detector's acceptance and the probability for a incoming neutron to be captured has been evaluated by comparing the integral of the two spectra shown in fig.9. Fig.9 shows the candidates neutrons (subtracted background) visible energy spectrum together with the simulated one made by generating $1 \cdot 10^7$ neutrons (kinetic energy spectrum given by [3] and [4], isotropic azimuthal distribution, zenithal distribution $\propto \cos^3 \theta$ [5], flux $\Phi_{neutron}(E > 20 \text{ MeV}) = 33$ neutron $s^{-1} m^{-2}$ [4]) on a surface $9 \times 6 m^2$ large placed 10 cm above the detector.

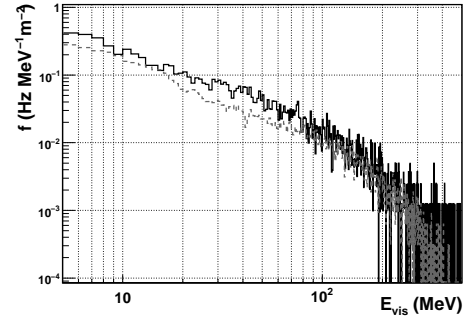


Fig. 9. Candidate Neutrons visible energy spectrum subtracted background (black line), simulated spectrum (grey dashed line)

Therefore we have estimated the neutron flux to be equal to:

$$\Phi_{neutron}(E > 10 \text{ MeV}) = 75 \pm 8 \text{ neutron } s^{-1} m^{-2}$$

$$\Phi_{neutron}(E > 20 \text{ MeV}) = 52 \pm 6 \text{ neutron } s^{-1} m^{-2}$$

VI. CONCLUSION

Using a detector made by a 1.2 tons of 0.1% Gd doped liquid scintillator and an active muon veto, located in the INFN Gran Sasso National Laboratory external site ($42^\circ 25' 11''$ N, $13^\circ 31' 2''$ E, altitude 970 m a.s.l.), the following results have been obtained:

1. the muon mean life in organic liquid scintillator $\tau = 2.125 \pm 0.015 \mu s$;
2. the stopping muons absolute rate for $E > 10 \text{ MeV}$: $R_\mu = 13.89 \pm 0.30$ (stat) ± 0.04 (syst) events s^{-1} ;
3. the atmospheric neutron flux: $\Phi_{neutron}(E > 10 \text{ MeV}) = 75 \pm 8$ neutron $s^{-1} m^{-2}$
 $\Phi_{neutron}(E > 20 \text{ MeV}) = 52 \pm 6$ neutron $s^{-1} m^{-2}$.

REFERENCES

- [1] N. A. Danilov *et al.* (2007), *Radiochemistry* 49, 281
- [2] I.R.Barabanov *et al.*, arXiv:0803.1577
- [3] T. Nakamura, *et al.* (2005) *Sequential Measurements of Cosmic-Ray Neutron Spectrum and Dose Rate at Sera Level in Sendai, Japan* *Journal of Nuc. Sc. and Tec.*, Vol.42, No.10, 843-853
- [4] M. Kowatari, *et al.* (2005) *Evaluation of the Altitude Variation of the Cosmic-ray Induced Environmental Neutrons in the Mt. Fuji Area* *Journal of Nuc. Sc. and Tec.*, Vol.42, No.6, 495-502
- [5] M. R. Moser *et al.* (2005) *Atmospheric Neutron Measurements in the 10-170 MeV Range*, 29th International Cosmic Ray Conference Pune 2, 421-424